Loss rate of ozone at inner surface of photoabsorption cells

H. Itoh[1], I. M. Rusinov[2], S. Suzuki[1], K. Teranishi[3] and N. Shimomura[3]

[1] *Department of Electrical, Electronic and Computer Engineering, Chiba Institute of Technology, Tsudanuma, Narashino, Chiba 275-0016, Japan*
[2] *Sofia University, Faculty of Physics, 5 James Bourchier Blvd., 1164 Sofia, Bulgaria*
[3] *Institute of Technology and Science, The University of Tokushima, Tokushima 770-8506 Japan*

An investigation was carried out on the surface loss rate of ozone in a cylindrical cells made of polytetrafluoroethylene (PTFE) and boron nitride. Each pipe is inserted into the photoabsorption cell which was made of stainless steel and used to the previous experiment. It is found that the surface loss rate of ozone decreased in the order boron nitride, PTFE and stainless steel. However, the loss rate of ozone in the gas phase was consistent with the value observed for the stainless steel cell indicating that the loss rate is independent of the cell material. The loss rate of ozone in the gas phase were obtained with high reproducibility and obtained values agreed with the previously obtained reaction rate coefficients of ozone by oxygen molecules and atoms of $2\times10^{-12}\exp(-10500/T)$ (cm^3/s) ($353 \leqq T < 423$ K) and $8\times10^{-22}\exp(-2840/T)$ (cm^3/s) ($293 < T \leqq 353$ K), respectively.

1. Introduction

Investigations on the surface loss rate of ozone were carried out by the HgI photoabsorption method using ultraviolet (UV) light with a wavelength of 253.7 nm [1][2]. The observed ozone concentration decreased exponentially with time, enabling us to evaluate the time constant of the decay curve. The time constant τ is equivalent to the effective lifetime of ozone in the cell. The observed effective lifetime increases with increasing in gas pressure from 20 to 500 Torr then reaches a peak at approximately atmospheric pressure and subsequently decreases inversely proportionally to the gas pressure. These experimental results are in good agreement with theoretical results derived by diffusion equation analysis of the ozone concentration in the cell. In the procedure, a third-kind boundary condition was adopted to solve the diffusion equation. Then we determined the equivalent diffusion coefficient of ozone in oxygen D_e (cm^2/s) together with the reflection coefficient of ozone at the inner surface of the cell R and the collisional reaction rate coefficient of ozone by oxygen k (cm^3/s).

2. Theoretical treatment of effective lifetime of ozone

In this study, the reciprocal of τ, which is the loss rate of ozone in the cell, is expressed by [1][2].

$$\frac{1}{\tau} = \frac{D_e}{p_0\Lambda^2} + kNp_0 = \frac{D_e}{p_0}\left\{\left(\frac{\nu_1}{a}\right)^2 + \left(\frac{q_1}{L}\right)^2\right\} + kNp_0 = \frac{1}{\tau_s} + \frac{1}{\tau_g}. \quad (2-1)$$

Here, the first and second terms on the right-hand side represent the ozone loss rate at the inner surface of the cell $1/\tau_s$ and that in the gas phase $1/\tau_g$, respectively. p_0 is the reduced gas pressure at 273.15 K, N is the number of oxygen molecules at 273.15 K at 1 Torr, Λ (cm) is the characteristic diffusion length of the cell, a (cm) is the radius of the cell, L (cm) is the length of the cell, ν_1 is the first root of the Bessel function ($xJ_1(x) - aJ_0(x)/\beta = 0$), and q_1 is the first root of the trigonometric function ($\cot x - \beta x/l = 0$), where $J_1(x)$ is the Bessel function of the first kind of order one, and $J_0(x)$ is the Bessel function of the first kind of order zero. β is a surface parameter and it is expressed as

$$\beta = \frac{\lambda(1+R)}{\sqrt{3}(1-R)}, \quad (2-2)$$

where, λ is the mean free path of ozone and R is the reflection coefficient of ozone on the inner surface of the cell. Detailed explanations of these parameters have already been given in previous papers [1][2].

3. Experimental apparatus and method

The simplified double beam method [2] based on the HgI photoabsorption method was used to monitor the ozone concentration in the UV region using light with a wavelength of 253.7 nm.

The temporal decrease in the ozone concentration was monitored using the cell illustrated at the center of Fig. 1. The cell was made of stainless steel and had a length of 200 mm and an inner diameter of 24 mm. In some measurements, a 200-mm-long PTFE or boron nitride cylinder with an inner diameter of 19 mm (PTFE) or 20 mm (boron nitride) was inserted in the stainless steel cell. Both ends of each cell were

sealed with quartz windows. The ozone generator was a small grounded stainless steel chamber equipped with a needle electrode that was filled with pure oxygen (99.999%). Ozone was formed by corona discharge under the application of a negative direct voltage to the needle electrode. After that, the ozone-oxygen mixture was transported to the photoabsorption cell. Both the cell and the ozone generator were connected to a turbomolecular pumping system which was used to evacuate the system to a pressure of 10^{-8} Torr or less.

Before the start of the measurement of the ozone concentration, the intensities of both the light through the cell in vacuum $I_{in}(0)$ and $I_{ref}(0)$ as the reference signal of $I_{in}(0)$ were monitored simultaneously. Subsequently, ozone was introduced into the cell then the intensities of the light transmitted through the cell $I_{out}(t)$ and the reference signal of the incident light intensity $I_{ref}(t)$ were monitored as functions of time t. When $I_{ref}(t)$ deviated from $I_{ref}(0)$, the ratio $I_{ref}(t)/I_{ref}(0)$ was employed to compensate for the deviation of the intensity $I_{in}(t)$ from $I_{in}(0)$. Therefore, we can obtain the corrected incident light intensity as the product of $[I_{ref}(t)/I_{ref}(0)]$ and $[I_{in}(0)]$. Then, the ozone concentration at a certain time t was obtained using [2]

$$c(t) = \frac{1}{\sigma p_0 NL} \ln\left[I_{in}(0) \frac{I_{ref}(t)}{I_{ref}(0)} \frac{1}{I_{out}(t)} \right] \ (\mathrm{cm}^{-3}) . \quad (3-1)$$

The temperature of the cell was monitored by attaching two thermocouples to the cell and using a datalogger. The temperature was controlled using a pair of flexible heaters which were wound around the cell with an insulator, and a temperature controller unit. In this experiment, the temperature was varied from 293 to 423 K.

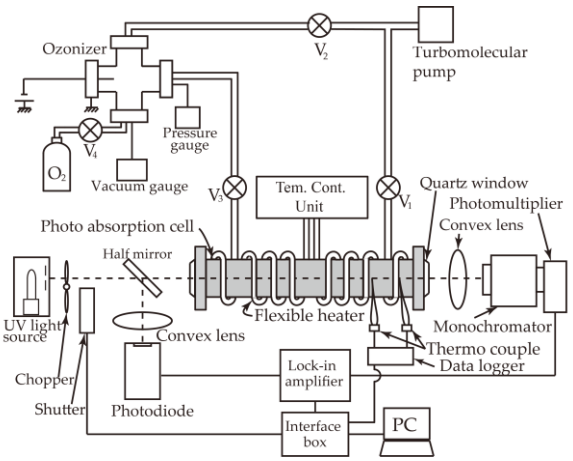

Fig. 1 Experimental apparatus. Ozone is formed in an ozonizer by corona discharge.

4. Experimental results and discussion

4.1 Observed effective lifetime of ozone

Each measurement was performed at least three times and the average effective lifetime of ozone at each gas pressure is plotted in Fig. 2. With increasing gas temperature, the effective lifetime against the gas pressure curve shifts downward while maintaining a similar dependence on the gas pressure. In Fig. 2, dotted straight lines represent proportional relationships between the effective lifetime and the gas pressure at low gas pressures. The intersection of each dotted line with the line $p_0 = 1$ Torr gives the reciprocal of the equivalent diffusion coefficient $1/D_e$ for each temperature. Moreover, the difference between the dotted straight lines and the curves fitting the experimental values corresponds to the reflection coefficient R at the surface of the cell for each cell temperature and gas pressure. In particular, for the new stainless steel surface, the change in the effective lifetime against the gas pressure curve is marked and the effective lifetime also depends on the aging effect is an effect as already described in the previous [1][2].

The observed effective lifetimes for the PTFE cell are plotted with squares and red lines against the gas pressure in Fig. 3. The effective lifetime of ozone in

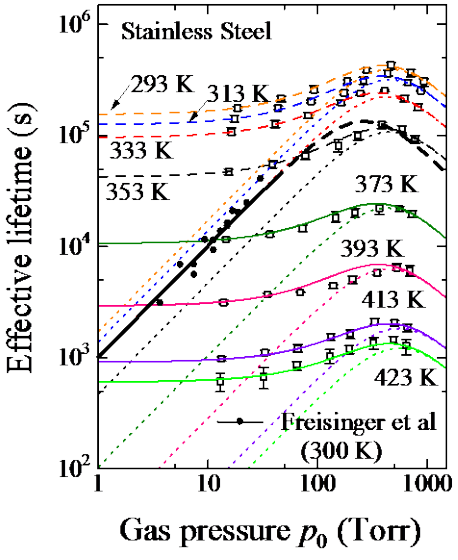

Fig. 2 Observed values of ozone effective lifetime against gas pressure. (Stainless steel)

PTFE cell is generally shorter than that in stainless steel cell. The observed effective lifetime of ozone in the boron nitride cell [3] is also shown in Fig. 3 as blue solid lines with triangles as a parameter of temperature.

4.2 Comparison of effective lifetime in cells of different materials

The effective lifetime in the boron nitride cell is shorter than those in the PTFE and stainless steel cells at low gas pressures of below 500 Torr. However, the peaks of effective lifetime in the boron nitride cell shifted to the highest gas pressures.

From the fitted curves shown in Fig. 3, D_e, k, and R were evaluated and are shown in Fig. 4. Among the three materials, D_e was the largest for the boron nitride cell, with similar results obtained for the stainless steel and PTFE cells. Both D_e and k increased with increasing cell temperature, wheseas, R remained constant for all three materials. The results indicate that the ozone loss rate was the largest at the surface of the boron nitride cell. The collisional reaction rate coefficient k which determines the ozone loss rate in the gas phase was similar for the three materials. The results lead to the reasonable conclusion that the loss rate of ozone in the gas phase is independent of the cell material.

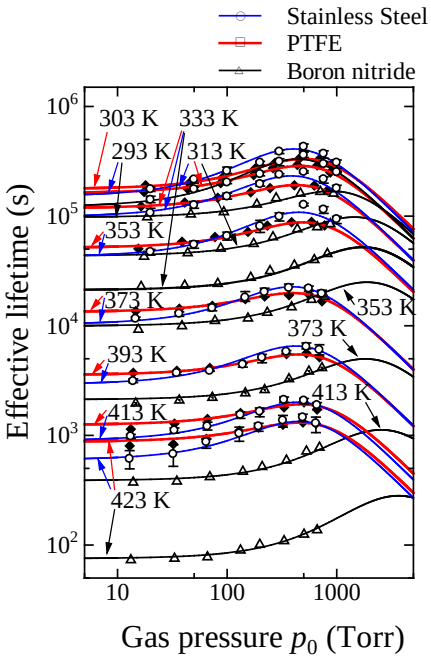

Fig. 3 Observed values of ozone effective lifetime against gas pressure. Black lines with circles: stainless steel, red lines with squares: PTFE, blue lines with triangles: boron nitride.

4.3 Discussion on effective lifetime of ozone against gas pressure

In Fig. 2, the closed circles with the solid black line show the results for the effective lifetime of ozone reported by Freisinger *et al*. [4]. They carried out their experiment on ozone formation by irradiating a UV laser into a container made of stainless steel (117 mmΦ diameter, 180 mm length) filled with O_2. Their effective lifetime curve against gas pressure is in agreement with our results at low pressures, i.e., the effective lifetime of ozone is proportional to the gas pressure. The upper limit of the effective lifetime is 4×10^4 s at a pressure of 30 Torr and ozone is considered to disappear only by diffusion up to this lifetime. Here, we assume that the ozone disappears as a result of collisions in the gas phase at pressures of higher than 30 Torr, and the broken black line in Fig. 2 was drawn assuming a reaction rate coefficient $k <$ of less than 4×10^{-25} cm^3/s. In other words, the value of the reaction rate coefficient 4×10^{25} cm^3/s was estimated as the minimum one under the above conditions. This result is acceptable with our experimental results.

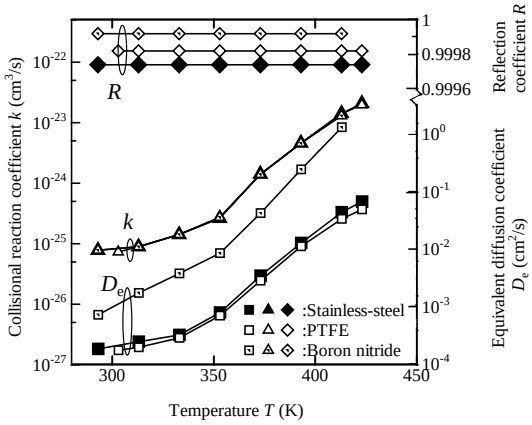

Fig. 4 Observed values of D_e, R and k against temperature in three kinds of materials.

4.4 Reaction rate coefficient of ozone by oxygen

Figure 5 shows Arrhenius plots of the reaction rate coefficients obtained from the experiment. All the plots are positioned on the pair of straight lines labelled with the reaction rate coefficients k_4 and k_5 which have a point of inflection at 353 K regardless of the cell. Although, it is reasonable that the reaction rate coefficient is determined only by the temperature, it is interesting fact that the ozone loss process varied with the temperature. Other reaction rate coefficients k_1, k_1', and k_2 are illustrated in the same figure.

The former coefficient corresponds to the decomposition of ozone by oxygen molecules,

expressed by

$$O_3 + O_2 \longrightarrow O + O_2 + O_2 \quad : \quad k_1 . \qquad (4 - 1)$$

The decomposition of ozone by oxygen atoms is expressed as

$$O_3 + O \longrightarrow O_2 + O_2\left(b^1\Sigma_g^+\right) \quad : \quad k_2 , \qquad (4 - 2)$$

$$O_3 + O \longrightarrow O_2 + O_2\left(a^1\Delta_g\right) \quad : \quad k_3 . \qquad (4 - 3)$$

Here, we use the reaction rate coefficient k_1 given by eq. (4 - 4) obtained by Hampson and Garvin [5], which has also been used by Eliasson and Kogelschatz [6], Freisinger *et al*. [4], Held and Peyrous [7], and others.

$$k_1 = 7.26\times10^{-10}\exp\left(-11400/T\right) \quad \left(\mathrm{cm^3/s}\right)$$
$$(200 - 1000\ \mathrm{K}) \qquad (4 - 4)$$

We also use the values of k_2 and k_3 reported by Eliasson and Kogelschatz [6] and Freisinger *et al*. [4], respectively, expressed

$$k_2 = 1.01\times10^{-11}\exp\left(-2300/T\right) \quad \left(\mathrm{cm^3/s}\right) \quad (4 - 5)$$
$$(220\ \mathrm{K} \leqq T \leqq 400\ \mathrm{K}) ,$$
$$k_3 = (0.00028 \sim 1.01)\times10^{-11}\exp\left(-2300/T\right) \quad \left(\mathrm{cm^3/s}\right)$$
$$(220\ \mathrm{K} \leqq T \leqq 400\ \mathrm{K}) . \qquad (4 - 6)$$

In Fig. 5, the solid line forming part of the broken line of k_1' was obtained experimentally by Zaslowsky *et al*. [8] ($k_1'=2.66\times10^{-8}\exp(-12154/T)$ ($\mathrm{cm^3/s}$)), and the broken line was extrapolated from their experimental values.

Our present values for the reaction rate coefficients k_4 and k_5 were obtained from Figs. 2 and 3 and are plotted as filled squares (■), open circles (○), and open triangles (△). These values are in good agreement and form two straight lines with different slopes corresponding to k_4 and k_5. The straight lines corresponding to k_4 and k_5 have the equations

$$k_4 = 8\times10^{-22}\exp\left(-2840/T\right) \quad \left(\mathrm{cm^3/s}\right) \qquad (4 - 7)$$
$$1/T > 2.83\times10^{-3}\ \mathrm{K^{-1}} \quad (T \leq 353\ \mathrm{K}),$$
$$k_5 = 2\times10^{-12}\exp\left(-10500/T\right) \quad \left(\mathrm{cm^3/s}\right) \qquad (4 - 8)$$
$$1/T < 2.83\times10^{-3}\ \mathrm{K^{-1}} \quad (T > 353\ \mathrm{K}).$$

Our values for the reaction rate coefficient k_4 obtained at temperatures below 353 K ($1/T > 2.83\times10^{-3}\ \mathrm{K^{-1}}$) form a line parallel to the straight lines of k_2 and k_3. The line of the reaction rate coefficient k_5 obtained in our results above 353 K ($1/T \leqq 2.83\times10^{-3}$) is parallel to the straight lines of k_1 and k_1'.

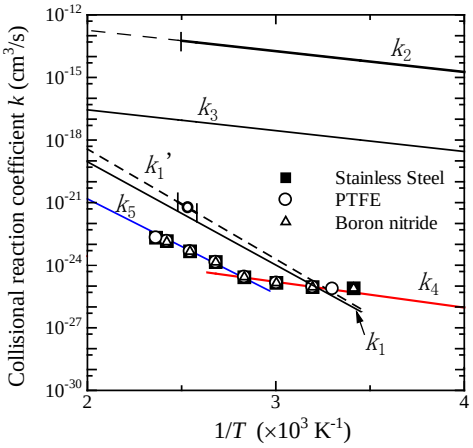

Fig. 5 Temperature dependence of reaction rate coefficients of ozone.

5. Conclusion

Three fundamental coefficients that describe the loss rate of ozone were determined as functions of gas pressure in stainless steel, PTFE and boron nitride cells over a wide range of temperatures. The obtained reaction rate coefficients k_4 and k_5 are considered to correspond to the loss rate of ozone induced by oxygen atoms and the loss rate of ozone by oxygen molecules, respectively.

6. References

[1] H. Itoh, I. M. Rusinov, T. Suzuki and S. Suzuki, Plasma Processes and Polymers, Vol.2, No.3, pp.227-231 (2005)

[2] H. Itoh, I. M. Rusinov, K. Omiya, and S. Suzuki, Ozone Science & Engineering, Vol.34, No.5, pp.370-377 (2012)

[3] K. Teranishi, N. Shimomura, S. Suzuki and H. Itoh, Plasma Sources Sci. Technol. 18 045011(2009)

[4] B. Freisinger, U. Kogelschatz, J. H. Schäfer, J. Uhlenbusch, and W. Viöl, Appl. Phys. B, Vol.49, pp.121-129 (1989)

[5] R. F. Hampson and D. Garvin, NBS Technical Note No.866, pp.1-113 (1975)

[6] B. Eliasson and U. Kogelschatz, Brown Boveri Konzernforschung, KLR-11C, Baden. (1986)

[7] B. Held and R. Peyrous, Eur. Phys. J. Appl. Phys., Vol.7, pp.73–86 (1998)

[8] J. A. Zaslowsky, H. B. Urbach, F. Leighton, R. J. Wnuk and J. A. Wojtowicz, J. Am. Chem. Soc., Vol.82, No.11, pp.2682-2686 (1960)